Polymer 50 (2009) 2806–2814

Contents lists available at ScienceDirect

Polymer

journal homepage: www.elsevier.com/locate/polymer

The role of introduced isolation groups in PVK-based nonlinear optical polymers: Enlarged nonlinearity, improved processibility, and enhanced thermal stability

Zhong'an Li [a], Gui Yu [b], Shoucheng Dong [a], Wenbo Wu [a], Yunqi Liu [b], Cheng Ye [b], Jingui Qin [a], Zhen Li [a,*]

[a] Department of Chemistry, Wuhan University, Wuhan 430072, China
[b] Organic Solids Laboratories, Institute of Chemistry, The Chinese Academy of Sciences, Beijing 100080, China

ARTICLE INFO

Article history:
Received 24 December 2008
Received in revised form
6 April 2009
Accepted 22 April 2009
Available online 3 May 2009

Keywords:
Poly(vinylcarbazole)
Nonlinear optics
Isolation groups

ABSTRACT

In this paper, a new series of PVK-based nonlinear optical (NLO) polymers were successfully synthesized, in which different isolation moieties (from the small to large size) were bonded to the NLO chromophore moieties. All the polymers were well characterized, and the obtained results demonstrated that the polymers exhibited improved solubility and processibility, and good optical transparency upon the introduction of the isolation groups, in addition to the enhanced NLO effects, further confirming that the linkage of isolation groups will not only boost the NLO properties of the resultant polymers to possibly high values, but also improve their processibility during the device manipulation process.

1. Introduction

Poly(N-vinylcarbazole) (PVK) is a well known polymer with high glass transition temperature (T_g), good processibility and high hole transport ability. Due to these advantages, it has been widely applied in many optical–electronics fields, such as photoconductors, photorefractive polymers (PR), organic light emitting diodes (OLEDs) and nonlinear optical (NLO) materials [1–10]. Usually, PVK was used as a good host in the above mentioned fields. As to the applications in the NLO area, although some exciting results have been achieved, the guest-host (PVK) system suffered from two problems: phase separation (chromophore recrystallization) and easily relaxation of the chromophore oriented dipoles. Thus, it was a good alternative choice to introduce the NLO chromophore moieties to the PVK backbone through covalent bonds, to address these two shortcomings [11–13]. However, the related reports were very scarce, possibly due to the lack of convenient synthetic approaches [14,15]. In 2001, our group has developed an easy postfunctionalization method to prepare an NLO chromophore-containing PVK (**PS1**, Chart 1), which exhibited good long-term stability of the NLO effect (the NLO activity remains unchanged at 120 °C for over 1000 h after a minor initial drop) [16]. However, the d_{33} value of the resultant polymer was not very high and its film-forming ability was relatively bad. Thus, to obtain PVK-based NLO materials with good performance, further efforts were still needed.

On the other hand, in the NLO research field, thanks to the great efforts of scientists, the $\mu\beta$ values of chromophores have been improved by up to 250 folds; the NLO effects of the polymers, however, were only enhanced several times due to the strong intermolecular dipole–dipole interactions in the polymeric system, which made the poling-induced noncentrosymmetric alignment of chromophores a daunting task [17–19]. Fortunately, the work of Jen and Dalton et al. have demonstrated that controlling the shape of chromophores through the introduction of isolation groups could be an efficient method to reduce the interaction and enhance the poling efficiency to increase the macroscopic NLO effects [20–23]. Based on their excellent job and according to the site isolation principle [24,25], since 2006, with the attempt to partially dissolve the above challenge: how to efficiently translate the large β values of the organic chromophores into high macroscopic NLO activities of polymers, we prepared different kinds of NLO polymers, in which the size of the isolation groups in NLO chromophore moieties was changed from small to very larger, and the obtained experimental results demonstrated that the macroscopic nonlinearity of NLO polymers could be boosted several times higher by bonding "suitable isolation groups" to the NLO chromophore moieties [26–35].

Thus, we considered that by introducing suitable spacers into the PVK polymeric system, the macroscopic nonlinearity would be enhanced. From this idea, we have prepared a series of PVK-based NLO polymers (**PS2**–**S5**, Chart 2) with different isolation spacers

* Corresponding author. Tel.: +86 27 62254108; fax: +86 27 68756757.
E-mail address: lizhen@whu.edu.cn (Z. Li).

0032-3861/$ – see front matter © 2009 Elsevier Ltd. All rights reserved.
doi:10.1016/j.polymer.2009.04.037

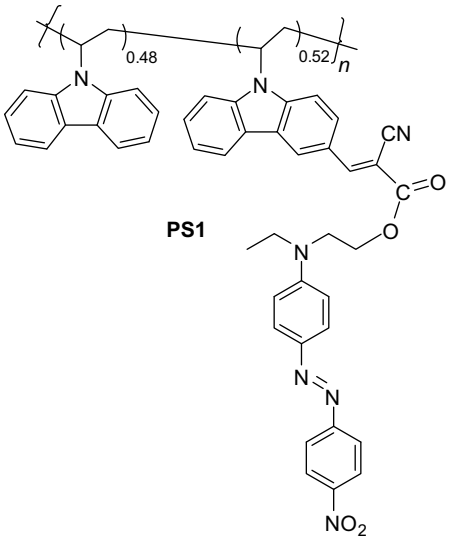

Chart 1.

bonded, in which the sulfonyl group was selected to use as the acceptors, due to its good optical transparency [36]. The results were consonant with our original idea, the resultant polymers exhibited enhanced NLO effects, and their long-term stabilities were also relatively good. Interestingly, some exciting phenomena were also observed, which were not expected at the very beginning of the polymer design:

1. while the isolation groups were introduced, the solubility and processibility of the polymers became much better;
2. the maximum absorption wavelength of the chromophore moieties in polymer solution was much blue-shifted (even up to 30 nm) in comparison with those of the free chromophore molecules in the same solvent. Generally, such hypsochromic shift may be attributed to the fact that the charge-transfer interaction between the electron acceptor and the tertiary amine-donor group was slightly reduced after incorporation of chromophore into polymer. The extent of blue-shifted maximum absorption in **PS2–S5** was really too big, much larger than our previous cases [26–31].

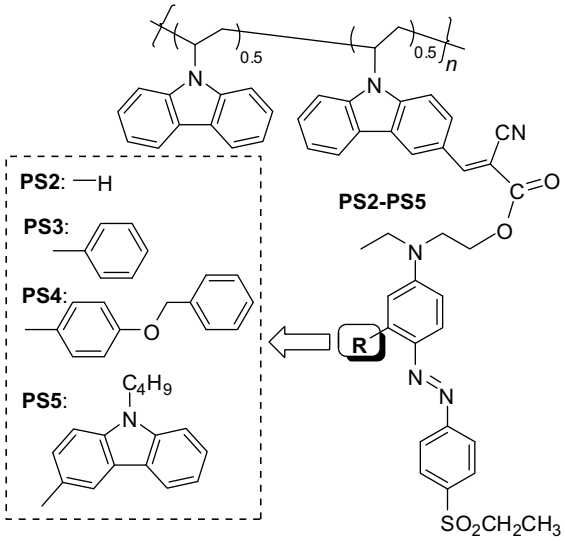

Chart 2.

These results were very encouraging and would surely benefit the practical application of the PVK-based polymers, however, these phenomena were not obviously observed in our other systems or found in the literatures. Were they special cases just for that system (**PS2–S5**) or common rule for PVK ones? To answer this question, and also improve the low poling efficiency and bad film-forming ability of **PS1**, we would like to introduce some isolation groups to the chromophore moieties of **PS1**, by applying the concept of "suitable isolation groups".

Therefore, in this article, a new series of PVK-based NLO polymers have been prepared successfully (Schemes 1 and 2), with the structure similar to those of the above mentioned polymers (**PS3–S5**) for comparison, while the only difference was that nitro-groups were used as the acceptors of chromophores instead of sulfonyl groups. The obtained experimental results were consistent with that of **PS2–S5**: after the suitable isolation groups (**BOP)** were introduced, the d_{33} value of the resultant polymer (**P2**) could be enhanced remarkably (up to 39.6 pm/V), two times higher than that of **PS1**, and its thermal stability of the NLO property was also better. In addition, the optical transparency and processibility of all the polymers were improved, in comparison with those of **PS1**, confirming that the above mentioned interesting phenomena were not a separate contingency, but might be universal. Herein, we would like to report the synthesis, characterization, and NLO properties of these PVK polymers.

2. Experimental section

2.1. Materials

Tetrahydrofuran (THF) was dried over and distilled from K–Na alloy under an atmosphere of dry nitrogen. *N*, *N*-Dimethylform amide (DMF) was dried over and distilled from CaH_2 under an atmosphere of dry nitrogen. Dichloromethane (CH_2Cl_2) was dried over anhydrous $CaCl_2$ and fresh distilled before use. Poly(*N*-vinylcarbazole) (PVK) was purchased from Aldrich, and its weight-averaged molecular weight was estimated to be 1.10×10^6. **PVK-CHO** (**P0**) was synthesized according to our previous work [16]. 3-Bromo-*N*-ethyl-*N*-(2-hydroxyethyl)aniline (**1**), 4-(benzyloxy)phenylboronic acid (**4**) and 3-*N*-(*n*-butyl) carbazole boronic acid (**6**) were synthesized according to our previous work [36]. All other reagents were used as received.

2.2. Instrumentation

^1H and ^{13}C NMR spectra were measured on a Varian Mercury300 spectrometer using tetramethylsilane (TMS; $\delta = 0$ ppm) as internal standard. The Fourier transform infrared (FTIR) spectra were recorded on a PerkinElmer-2 spectrometer in the region of 3000–400 cm^{-1} on NaCl pellets. UV-visible spectra were obtained using a Shimadzu UV-2550 spectrometer. Gel permeation chromatography (GPC) was used to determine the molecular weights of polymers. GPC analysis was performed on a Waters HPLC system equipped with a 2690D separation module and a 2410 refractive index detector. Polystyrene standards were used as calibration standards for GPC. DMF was used as eluent, and the flow rate was 1.0 mL/min. EI-MS spectra were recorded with a Finnigan PRACE mass spectrometer. Elemental analyses were performed by a CARLOERBA-1106 micro-elemental analyzer. Thermal analysis was performed on NETZSCH STA449C thermal analyzer at a heating rate of 10 °C/min in nitrogen at a flow rate of 50 cm^3/min for thermogravimetric analysis (TGA). The thermal transitions of the

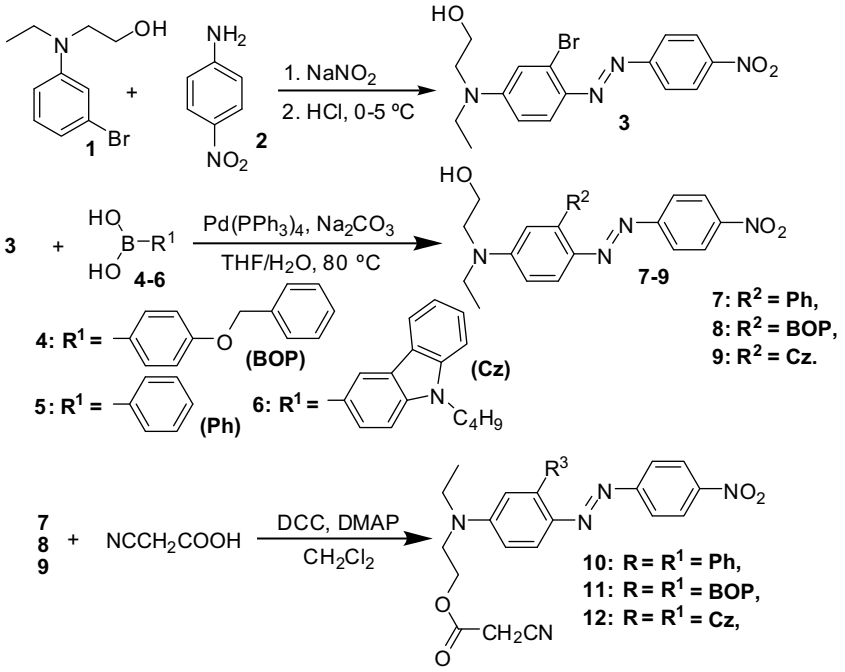

Scheme 1.

polymers were investigated using a METTLER differential scanning calorimeter DSC822e under nitrogen at a scanning rate of 10 °C/min. The thermometer for measurement of the melting point was uncorrected. The thickness of the films was measured with an Ambios Technology XP-2 profilometer.

2.3. Synthesis of chromophore 3

4-Nitroaniline (**2**) (0.59 g, 4.28 mmol) was dissolved in a water solution of 35% hydrochloric acid. The mixture was cooled to 0–5 °C in an ice bath, and then a solution of sodium nitrite (0.34 g, 5.00 mmol) in water was added to the above cooled solution dropwise. After stirred below 5 °C for 15 min, a solution of **1** (1.00 g, 4.10 mmol) in ethanol was added slowly. The mixture was left in the ice bath for another 1 h, some sodium bicarbonate was added to adjust the pH value to about 7.0. The reaction mixture was stirred for another 0.5 h, the red precipitate was filtered, washed with water. The crude product was purified by recrystallization from ethanol/water to afford deeply red powder (1.46 g, 90.7%). Mp = 140–141 °C. ^{1}H NMR ($CDCl_3$) δ (ppm): 1.25 (t, J = 7.5 Hz, 3H, -CH_2CH_3), 3.50–3.61 (m, 4H, -N-CH_2-), 3.90 (t, J = 5.7 Hz, 2H, -O-CH_2-), 6.69 (dd, J = 2.4, 9.3 Hz, 1H, ArH), 7.04 (d, J = 2.1 Hz, 1H, ArH), 7.78 (d, J = 8.7 Hz, 1H, ArH), 7.96 (d, J = 8.7 Hz, 2H, ArH), 8.30 (d, J = 8.7 Hz, 2H, ArH).

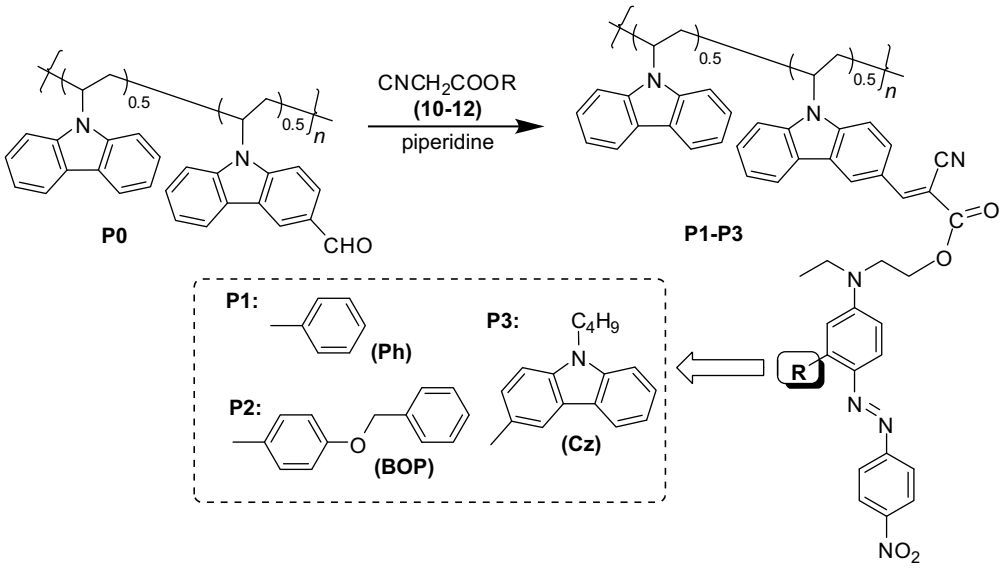

Scheme 2.

2.4. General procedure for the synthesis of chromophores 7, 8 and 9

A mixture of chromophore **3** (1.00 equiv), the boronic acid **4**, **5** or **6** (1.05–1.10 equiv), sodium carbonate (10.0 equiv), THF (the concentration of chromophore **3** is about 0.05 M)/water (3:1 in volume), and tetrakis(triphenylphosphine)palladium ($Pd(PPh_3)_4$) (3–5 mol%) was carefully degassed and charged with nitrogen. The reaction was stirred at 80 °C for about 30 h. After it was cooled to room temperature, the organic layer was separated, dried over sodium sulfate, and evaporated to dryness. The crude product was purified by recrystallization or column chromatography.

2.4.1. Chromophore 7

3 (393 mg, 1.00 mmol), **5** (134 mg, 1.10 mmol). Purified by recrystallization from ethanol/acetone to afford deeply red powder (330 mg, 84.6%). Mp = 169–170 °C. ^{1}H NMR ($CDCl_3$) δ (ppm): 1.30 (t, J = 6.9 Hz, 3H, -CH_3), 3.5–3.7 (m, 4H, -N-CH_2-), 3.94 (br, s, 2H, -O-CH_2-), 6.82 (m, 2H, ArH), 7.4–7.6 (m, 5H, ArH), 7.72 (d, J = 9.0 Hz, 2H, ArH), 7.94 (d, J = 8.4 Hz, 1H, ArH), 8.22 (d, J = 9.0 Hz, 2H, ArH).

2.4.2. Chromophore 8

3 (250 mg, 0.64 mmol), **4** (160 mg, 0.70 mmol). Purified by recrystallization from ethanol/acetone to afford deeply red powder (279 mg, 88.0%). Mp = 128–129 °C. ^{1}H NMR ($CDCl_3$) δ (ppm): 1.27 (t, J = 7.2 Hz, 3H, -CH_3), 3.5–3.7 (m, 4H, -N-CH_2-), 3.94 (br, s, 2H, -O-CH_2-), 3.94 (s, 2H, -O-CH_2Ph), 6.78 (m, 2H, ArH), 7.04 (d, J = 8.7 Hz, 2H, ArH), 7.3–7.5 (m, 7H, ArH), 7.73 (d, J = 9.0 Hz, 2H, ArH), 7.94 (d, J = 9.0 Hz, 1H, ArH), 8.23 (d, J = 8.7 Hz, 2H, ArH).

2.4.3. Chromophore 9

3 (500 mg, 1.27 mmol), **6** (336 mg, 1.33 mmol). Purified by column chromatography on silica gel using ethyl acetate/petroleum ether (2/1) as eluent to afford deeply red solid (587 mg, 86.5%). Mp = 98–100 °C. ^{1}H NMR ($CDCl_3$) δ (ppm): 0.95 (t, J = 7.5 Hz, 3H, -CH_3), 1.31 (m, 3H, -CH_3), 1.45 (m, 2H, -CH_2-), 1.91 (m, 2H, -CH_2-), 3.61–3.75 (m, 4H, -N-CH_2-), 3.93 (br, s, 2H, -O-CH_2-), 4.36 (t, J = 7.2 Hz, 2H, -N-CH_2-), 6.83 (br, s, 1H, ArH), 6.93 (s, 1H, ArH), 7.22 (m, 1H, ArH), 7.47 (m, 3H, ArH), 7.61 (d, J = 8.4 Hz, 1H, ArH), 7.76 (d, J = 8.4 Hz, 2H, ArH), 8.00 (m, 2H, ArH), 8.15 (d, J = 8.4 Hz, 2H, ArH), 8.22 (s, 1H, ArH).

2.5. General procedure for the synthesis of chromophores 10, 11 and 12

Chromophores **7**, **8**, or **9** (1.00 equiv), dicyclohexylcarbodiimide (DCC) (1.30–1.50 equiv), cyanoacetic acid (1.20–1.50 equiv), 4-(*N*,*N*-dimethyl)aminopyridine (DMAP) (0.20 equiv) were dissolved in proper dry CH_2Cl_2 and stirred at room temperature for 20 h. The precipitate was filtered and the crude product was purified by column chromatography.

2.5.1. Chromophore 10

7 (150 mg, 0.38 mmol), cyanoacetic acid (42 mg, 0.48 mmol). Purified by column chromatography on silica gel using ethyl acetate/petroleum ether (1/1) as eluent to afford red solid (113 mg, 65.0 %). Mp = 107–109 °C. IR (thin film), υ (cm^{-1}): 1754 (C = O), 1518, 1339 (-NO_2). ^{1}H NMR ($CDCl_3$) δ (ppm): 1.29 (t, J = 7.2 Hz, 3H, -CH_3), 3.44 (s, 2H, -CH_2CN), 3.58 (q, J = 7.2 Hz, 2H, -NCH_2-), 3.77 (t, J = 6.3 Hz, 2H, -NCH_2-), 4.46 (t, J = 6.0 Hz, 2H, -O-CH_2-), 6.78 (m, 2H, ArH), 7.4–7.6 (m, 5H, ArH), 7.74 (d, J = 9.0 Hz, 2H, ArH), 7.95 (d, J = 9.3 Hz, 1H, ArH), 8.24 (d, J = 9.0 Hz, 2H, ArH). ^{13}C NMR ($CDCl_3$) δ (ppm): 12.59, 24.83, 46.05, 48.57, 63.99, 111.65, 112.68, 117.99, 123.23, 124.88, 127.84, 130.96, 139.62, 141.23, 146.47, 147.60, 150.93, 156.95, 163.03. MS (EI), m/z [M^+]: 457.2, calcd: 457.2. $C_{25}H_{23}N_5O_4$ (EA) (%, found/calcd): C, 65.71/65.63; H, 5.52/5.07; N, 14.83/15.31. UV-Vis (DMF, 2.5×10^{-5} mol/L): λ_{max}: 494 nm; ε_{max}: 2.00×10^4 mol^{-1} L cm^{-1}.

2.5.2. Chromophore 11

8 (149 mg, 0.30 mmol), cyanoacetic acid (39 mg, 0.45 mmol). Purified by column chromatography on silica gel using ethyl acetate/petroleum ether (1/1) as eluent to afford red solid (143 mg, 84.6%). Mp = 115–116 °C. IR (thin film), υ (cm^{-1}): 1754 (C = O), 1318, 1339 (-NO_2). ^{1}H NMR ($CDCl_3$) δ (ppm): 1.28 (t, J = 7.2 Hz, 3H, -CH_3), 3.43 (s, 2H, -CH_2CN), 3.58 (q, J = 7.5 Hz, 2H, -NCH_2-), 3.77 (t, J = 6.6 Hz, 2H, -NCH_2-), 4.45 (t, J = 5.9 Hz, 2H, -O-CH_2-), 5.16 (s, 2H, -CH_2Ph), 6.77 (m, 2H, ArH), 7.05 (d, J = 9.0 Hz, 2H, ArH), 7.3–7.5 (m, 7H, ArH), 7.74 (d, J = 8.7 Hz, 2H, ArH), 7.92 (d, J = 9.6 Hz, 1H, ArH), 8.23 (d, J = 9.0 Hz, 2H, ArH). ^{13}C NMR ($CDCl_3$) δ (ppm): 12.62, 24.83, 46.04, 48.56, 63.99, 70.32, 111.41, 112.44, 112.85, 114.30, 118.05, 123.22, 124.89, 127.76, 128.29, 128.87, 132.21, 137.15, 141.27, 146.01, 147.56, 150.98, 157.02, 158.81, 163.05. MS (EI), m/z [M^+]: 563.0, calcd: 563.2. $C_{32}H_{29}N_5O_5$ (EA) (%, found/calcd): C, 67.99/68.19; H, 5.32/5.19; N, 12.31/12.43. UV-Vis (DMF, 2.5×10^{-5} mol/L): λ_{max}: 497 nm; ε_{max}: 2.52×10^4 mol^{-1} L cm^{-1}.

2.5.3. Chromophore 12

9 (250 mg, 0.47 mmol), cyanoacetic acid (50 mg, 0.57 mmol). Purified by column chromatography on silica gel using chloroform/ethyl acetate (1/1) as eluent to afford red solid (235 mg, 82.3%). Mp = 96–99 °C. IR (thin film), υ (cm^{-1}): 1750 (C = O), 1526, 1334 (-NO_2). ^{1}H NMR ($CDCl_3$) δ (ppm): 0.99 (t, J = 7.5 Hz, 3H, -CH_3), 1.31 (t, J = 6.9 Hz, 3H, -CH_3), 1.45 (m, 2H, -CH_2-), 1.93 (m, 2H, -CH_2-), 3.44 (s, 2H, -CH_2CN), 3.61 (q, J = 6.9 Hz, 2H, -NCH_2-), 3.82 (t, J = 6.3 Hz, 2H, -NCH_2-), 4.36 (t, J = 6.9 Hz, 2H, -N-CH_2-), 4.49 (t, J = 7.2 Hz, 2H, -O-CH_2-), 6.80 (d, J = 9.0 Hz, 1H, ArH), 6.92 (s, 1H, ArH), 7.22 (m, 1H, ArH), 7.45 (m, 3H, ArH), 7.63 (d, J = 8.4 Hz, 1H, ArH), 7.76 (d, J = 9.0 Hz, 2H, ArH), 7.99 (d, J = 9.0 Hz, 1H, ArH), 8.07 (d, J = 7.8 Hz, 1H, ArH), 8.18 (d, J = 8.7 Hz, 2H, ArH), 8.24 (s, 1H, ArH). ^{13}C NMR ($CDCl_3$) δ (ppm): 12.69, 14.15, 20.84, 24.85, 31.45, 43.27, 46.08, 48.58, 64.03, 108.00, 109.16, 111.29, 113.02, 118.08, 119.34, 120.45, 122.69, 123.02, 123.20, 124.89, 126.08, 128.99, 130.08, 140.35, 141.14, 141.54, 147.21, 147.47, 150.99, 157.12, 163.08. MS (EI), m/z [M^+]: 602.0, calcd: 602.3. $C_{32}H_{29}N_5O_5$ (EA) (%, found/calcd): C, 69.33/69.75; H, 5.56/5.69; N, 13.98/13.94. UV-Vis (DMF, 2.5×10^{-5} mol/L): λ_{max}: 498 nm; ε_{max}: 3.00×10^4 mol^{-1} L cm^{-1}.

2.6. General procedure for synthesis of polymers P1–P3

2.6.1. PVK-CHO (P0)

PVK-CHO (P0) (1.00 equiv) was dissolved in DMF (0.08 M-CHO), then a solution of one of chromophores **10**–**12** (2.60–3.00 equiv) dissolved in THF and a catalytic amount of piperidine was added under an atmosphere of dry nitrogen. The reaction mixture was stirred at 45 °C for 48 h, then dropped into methanol. The obtained orange precipitate was filtered and washed with methanol for several times. The resultant product was collected and dried under vacuum at 40 °C.

2.6.2. P1

P0 (31 mg), **10** (90 mg, 0.20 mmol). Red powder (54 mg, 55.6%). $M_w = 8.07 \times 10^5$, $M_w/M_n = 1.17$ (GPC, polystyrene calibration). IR (thin film), υ (cm^{-1}): 2218 (CN), 1723 (C = O), 1674, 748, 723 (carbazole), 1518, 1339 (-NO_2). ^{1}H NMR (DMSO-d_6) δ (ppm): 1.0–1.4 (-CH_3), 3.6–4.2 (-CH_2-), 6.5–7.0 (ArH), 7.0–7.8 (ArH), 7.8–8.2 (ArH). UV-Vis (DMF, 0.02 mg/mL): λ_{max} (nm): 490 nm; UV-Vis (film): λ_{max} (nm): 482 nm.

2.6.3. P2

P0 (32 mg), **11** (113 mg, 0.20 mmol). Red powder (58 mg, 50.0%). $M_w = 7.41 \times 10^5$, $M_w/M_n = 1.31$ (GPC, polystyrene calibration). IR (thin film), υ (cm^{-1}): 2217 (CN), 1727 (C=O), 1675, 748, 727 (carbazole), 1518, 1339 (-NO_2). ^{1}H NMR (DMSO-d_6) δ (ppm): 1.0–1.4 (-CH_3), 3.6–4.2 (-CH_2-), 4.8–5.0 (-OCH_2Ph), 6.5–6.9 (ArH), 7.0–7.7 (ArH), 7.8–8.2 (ArH). UV-Vis (DMF, 0.02 mg/mL): λ_{max} (nm): 491 nm; UV-Vis (film): λ_{max} (nm): 482 nm.

2.6.4. P3

P0 (42 mg), **12** (169 mg, 0.28 mmol). Red powder (69 mg, 43.7%). $M_w = 7.14 \times 10^6$, $M_w/M_n = 1.27$ (GPC, polystyrene calibration). IR (thin film), υ (cm^{-1}): 2217 (CN), 1723 (C=O), 1674, 745, 723 (carbazole), 1514, 1134 (-SO_2). ^{1}H NMR (DMSO-d_6) δ (ppm): 0.7–0.9 (-CH_3), 1.0–1.4 (-CH_3), 1.4–1.6 (-CH_2-), 1.8–2.0 (-CH_2-), 3.7–4.0 (-NCH_2-), 4.1–4.4 (-OCH_2 and -$CNCH_2$), 4.6–4.8 (-OCH_2-), 6.4–6.6 (ArH), 6.6–6.9 (ArH), 6.9–7.1 (ArH), 7.2–7.6 (ArH), 7.6–7.8 (ArH), 7.9–8.2 (ArH). UV-Vis (DMF, 0.02 mg/mL): λ_{max} (nm): 492 nm; UV-Vis (film): λ_{max} (nm): 487 nm.

2.6.5. Preparation of polymer thin films

The polymers were dissolved in DMF (concentration ~8 wt%), and the solutions were filtered through syringe filters. Polymer films were drop-coated onto indium-tin-oxide (ITO)-coated glass substrates (22 × 22 mm), which were cleaned by *N*,*N*-dimethylformamide, acetone, distilled water and THF sequentially in ultrasonic bath before use. Residual solvent was removed by heating the films in a vacuum oven at 40 °C.

2.6.6. NLO measurement of poled films

The second-order optical nonlinearity of the polymers was determined by in-situ second harmonic generation (SHG) experiment using a closed temperature-controlled oven with optical windows and three needle electrodes. The films were kept at 45 °C to the incident beam and poled inside the oven, and the SHG intensity was monitored simultaneously. Poling conditions were as follows: temperature: different for each polymer (Table 1); voltage: 7.7 kV at the needle point; gap distance: 0.8 cm. The SHG measurements were carried out with a Nd:YAG laser operating at a 10 Hz repetition rate and an 8 ns pulse width at 1064 nm. A Y-cut quartz crystal served as the reference.

2.6.6.1. General NLO test procedure. After the film was placed in the oven, the oven was heated under the control of one computer, and the temperature increased from room temperature to the predetermined one (generally 10 °C above the glass transition temperature). At the same time, one beam of laser irradiated on the film to produce the SHG signal, which was measured by an optical power meter detector (Beijing Bingsong Photon Technological Corporation, China). The detector was connected to a computer, and there was a light filter in front of the detector, only the light with the wavelength of 532 nm could be collected. After the maximum signal (I_s) was captured, the SHG signal of a Y-cut quartz crystal (I_q) was tested as the reference. Then, the heating of the oven was stopped, and the power of the laser was turned off.

Table 1
Polymerization results and characterization data.

No.	Yield (%)	M_w[a] $\times 10^5$	M_w/M_n[a]	λ_{max}[b] (nm)	T_g[c] (°C)	T_d[d] (°C)	T_e[e] (°C)	l_s[f] (μm)	d_{33}[g] (pm/V)	$d_{33\,(\infty)}$[h] (pm/V)	Φ[i]
P1	55.6	8.07	1.17	490 (494)	140	290	154	0.71	29.4	3.5	0.11
P2	50.0	7.41	1.28	491 (498)	154	274	171	0.87	39.5	4.6	0.19
P3	43.7	7.14	1.32	492 (498)	158	307	170	0.67	34.0	3.9	0.17

[a] Determined by GPC in DMF on the basis of a polystyrene calibration.
[b] The maximum absorption wavelength of polymer solutions in THF, while the maximum absorption wavelength of the corresponding small chromophore molecules in diluted THF solutions is given in the parentheses.
[c] Glass transition temperature (T_g) of polymers detected by the DSC analyses under nitrogen at a heating rate of 10 °C/min.
[d] The 5% weight loss temperature of polymers detected by the TGA analyses under argon at a heating rate of 10 °C/min.
[e] The best poling temperature.
[f] Film thickness.
[g] Second harmonic generation (SHG) coefficient.
[h] The nonresonant d_{33} values calculated by using the approximate two-level model.
[i] Order parameter $\Phi = 1 - A_1/A_0$, A_1 and A_0 are the absorbance of the polymer film after and before corona poling, respectively.

3. Results and discussion

3.1. Synthesis and characterizations

The overall pathway of the monomer synthesis was presented in Scheme 1. Through the normal azo coupling reaction, chromophore **3** was easily prepared in high yield, and it underwent the followed Suzuki reactions [37], with different boronic acids, including phenyl boronic acid (**4**), 1-benzyloxy-4-(boronic acid)-benzene (**5**) and 3-*N*-(*n*-butane) carbazole boronic acid (**6**), to yield the corresponding chromophores **7–9** with different size of isolation groups in moderate yields. Finally, cyanoacetylated chromophores **10–12** were prepared by the reactions of chromophores **7–9** with cyanoacetic acid under mild conditions (Scheme 1) [38].

It was easily seen that PVK-based NLO polymers, **P1–P3**, were conveniently obtained by Knoevenagel condensation reactions between the partially formylated PVK (**P0**) and their corresponding chromophores with different isolation moieties [16]. Thus, **P1–P3** possessed similar structures (the same polymeric main chain and the same loading molar concentration of the NLO chromophore), the only different point was the different size of the isolation groups bonded to the chromophore moieties.

The chromophores and polymers were characterized by spectroscopic methods, and all give satisfactory spectral data (see Experimental section and Table 1 for detailed analysis data). As shown in the IR spectra of polymers (Fig. 1), an apparently strong absorption band appeared at 1693 cm^{-1} in **P0**, which was in the frequency range expected for the carbonyl stretching vibration of

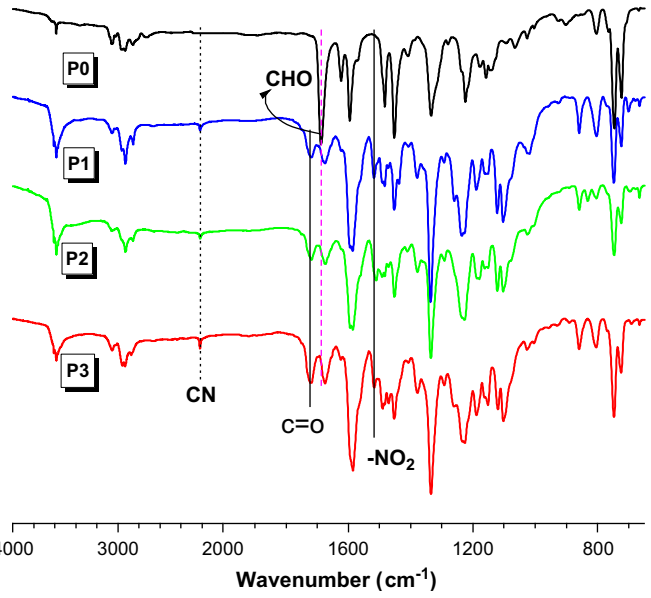

Fig. 1. IR spectra of polymers **P0–3**.

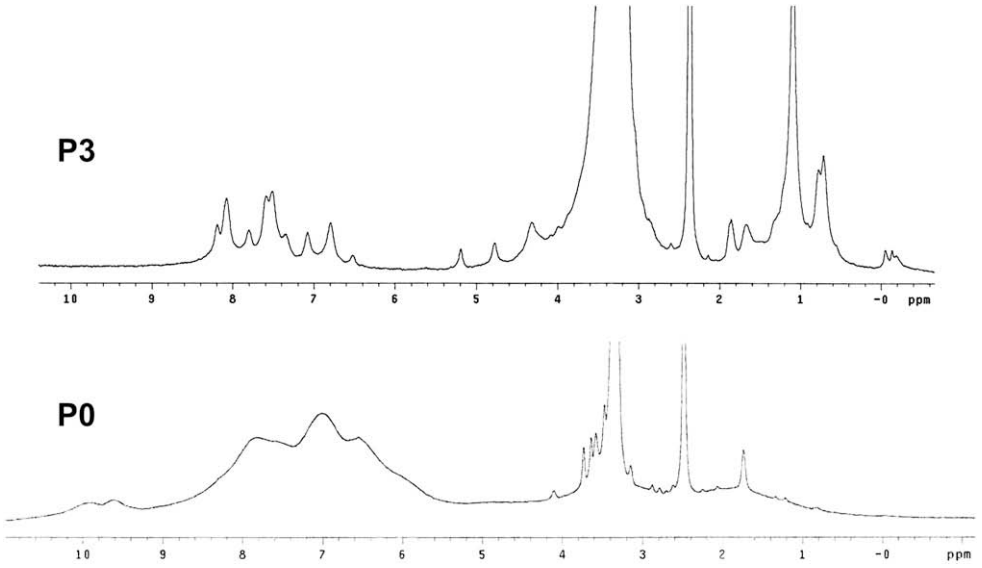

Fig. 2. ^{1}H NMR spectra of polymers **P0** and **P3** in DMSO-d_6.

an aromatic aldehyde, confirming that the high concentration of formyl groups was introduced into the carbarzole ring by Vilsmeier reaction. After further functionalized with cyanoacetylated chromophores **10**–**12**, these bands of polymers **P1**–**3** disappeared and new absorption bands at 1750 and 2220 cm^{-1} appeared, which were contributed by the carbonyl stretching vibration of a conjugated carboxylic ester and the nitrile stretching vibration respectively. Moreover, the new appearance of nitro group absorption was at about 1516 cm^{-1}. All these changes indicated that the functional chromophores were successfully added to the PVK backbone.

It is well known that the formyl groups and the active methylene species in the cyanoacetate possessed high reactivity towards the Knoevenagel condensation reaction, so under the similar conditions as our previous work [36], the postfunctionalization reactions of **P0** with chromophores **10–12** proceeded easily and completely. In the ^{1}H NMR spectra of all the polymers, the chemical shifts were consistent with the proposed polymer structure (Scheme 2), and the absorption peak of the aldehyde groups disappeared, proving the almost complete conversion of the formyl groups of **P0** to chromophore-functionalized PVK-based polymers, **P1–P3**. Fig. 2 demonstrated the spectra of **P0** and **P3** for example.

All the polymers were soluble in polar organic solvents, such as DMF, DMSO, and NMP. Also, for good comparison, we re-synthesized the polymer **PS1**, which, however, exhibited bad solubility, and nearly could not be handled for any test. On the contrary, under the same synthetic conditions, the obtained polymers (**P1**–**P3**) demonstrated much better solubility, similar as observed previously in **PS2**–**S5**. This should be ascribed to the presence of the bonded isolation groups, which might efficiently suppress the polymer inter-chain entanglements and benefit the polymer chain to extend in solvents [39]. Furthermore, the solubility seemed to be improved much better accompanying with the enlargement of the isolation groups, partly confirming the above explanation.

The UV-Vis absorption spectra of polymers in DMF solutions were shown in Fig. 3, and the maximum absorption wavelength for the π–π^* transition of the azo moieties in them was listed in the Experimental section and Table 1. All of the polymers exhibited weak absorption bands of the carbazole group at about 324 nm. It was easily seen that the maximum absorption wavelength of the polymers was almost the same, indicating that the introduction of the different isolation groups to the donor side of the chromophore molecules did not affect their electronic structure properties at a large extent. Thus, it was reasonable for us to focus our eyes on the relationship between the size of the isolation groups and the resultant NLO properties of the PVK-based polymers.

As discussed in the introduction part, the maximum absorption wavelengths of the chromophore moieties in **PS2**–**S5** in solutions were much blue-shifted (up to 30 nm) in comparison with those of the free chromophore molecules in the same solvent, and the maximum absorption wavelengths of the polymer films were further blue-shifted (about 10 nm), with related to the isolation effects [20]. Here, similar phenomena were observed in this polymeric system, however, the blue-shifted extent of **P1**–**3** (4 ~ 7 nm) was not as large as those of **PS2**–**S5**. Considering the structure of **P1**–**3** was very similar to that of **PS2**–**S5**, the much less blue-shifted maximum absorption of **P1**–**3** should be due to the different

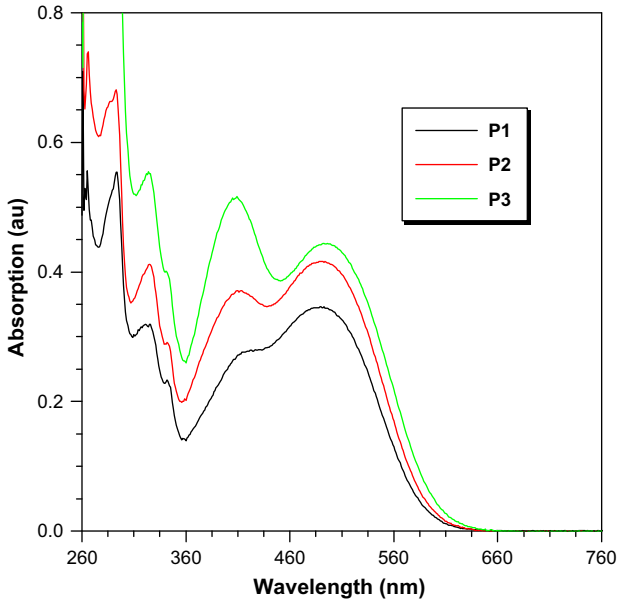

Fig. 3. UV-Vis spectra of DMF solutions of polymers **P1–3** (0.02 mg/mL).

acceptors used. As we know, the electron-pulling ability of nitro-groups was much larger than that of sulfonyl groups, thus, the aggregation of the former would be much serious than that of the latter. Therefore, the same isolation groups led to different isolation effects, and the better blue-shifted extent of **PS2**–**S5** should be caused by the much efficient reduction of the chromophore aggregation.

The molecular weights of polymers were determined by gel permeation chromatography (GPC) with DMF as an eluent and polystyrene standards as calibration standards, and all the results were summarized in Table 1. **P1**–**P3** possessed similar molecular weights, indicating that the reaction conditions were mild and PVK backbone was stable during the reaction process. The polymers were thermolytically resistant, with their TGA thermograms shown in Fig. 4, and the 5% weight loss temperature of polymers were listed in Table 1. The results showed that all the polymers exhibited good thermal stability up to 300 °C. **P2** was not so stable as **P1** and **P3**, possibly due to the unstable benzyl groups. The glass transition temperature (T_g) of the polymers was investigated using a differential scanning calorimeter (Table 1), all the polymers generally have moderate T_g about 155 °C, derived from the rigid mother polymer, PVK. All the thermal results revealed the superiorities of PVK used as polymeric backbone.

3.2. NLO properties

To evaluate the NLO activity of the polymers, their poled thin films were prepared. The most convenient technique to study the second-order NLO activity is to investigate the second harmonic generation (SHG) processes characterized by d_{33}, an SHG coefficient. The method for the calculation of the SHG coefficients (d_{33}) for the poled films has been reported in our previous papers [40–44]. From the experimental data, the d_{33} values of **P1–P3** are calculated at fundamental wavelength of 1064 nm (Table 1).

As we expected, **P1–P3** demonstrated different NLO properties, due to their different structures, especially the different introduced isolation groups linked to the chromophore moieties in the donor side. To study the NLO results visually, we compared the d_{33} values of the polymers using that of **P1** as reference (Fig. 5A). As expected,

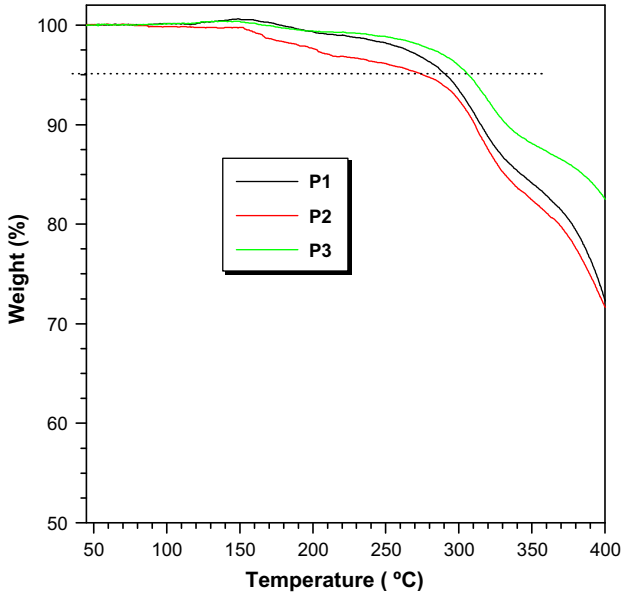

Fig. 4. TGA thermograms of **P1–P3**, measured in nitrogen at a heating rate of 10 °C/min.

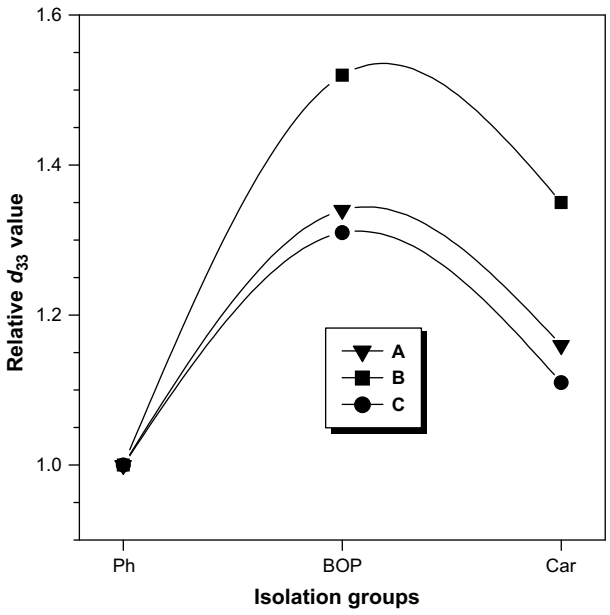

Fig. 5. A) Comparison of the d_{33} values of the polymers. (B) Comparison of the calculated d_{33} values, which were obtained by using the tested d_{33} values of the polymers dividing the concentration of the active chromophore moieties of the polymers. (C) Comparison of the calculated $d_{33(\infty)}$ values of the polymers, according to the approximate two-level model, using **P1** as the reference.

the d_{33} values were not always increasing as the isolation groups enlarged from phenyl ring to carbazole moieties, and there was also a suitable group (**BOP** moieties in **P2**) present, similar phenomenon as our previous work [26–35], further proving the concept of "suitable isolation groups": for a given chromophore moiety and given linkage position, there should be a suitable isolation group present to boost its microscopic β value to possible higher macroscopic NLO property efficiently. When the isolation groups changed from **Ph** to the **BOP** groups, the d_{33} value of **P2** (39.6 pm/V) was enhanced 1.34 times that of **P1**. While the size of isolation groups was further enlarged (**Car** groups in **P3**), the tested d_{33} value still kept 34.0 pm/V, 1.16 times that of **P1**. In general, the d_{33} values of all the polymers (**P1**–**3**), here, increased efficiently in comparison with that of **PS1** (20 pm/V), due to the introduced isolation groups to restrain the intermolecular electrostatic dipole–dipole interactions, indicating that it was an efficient method to enhance the poling efficiency of high-T_g polymers.

Since the introduction of different isolation groups would result in the diluted concentration of the active chromophore moieties in the polymers, we used the tested d_{33} values dividing the molar concentrations of the active chromophore moieties, then compared the results again with that of **P1** as the reference (Fig. 5B). Thus, it was easily seen that the trend of the two curves (the labeled A and B) was nearly the same, and **BOP** was also the better isolation group. Considering there might be some resonant enhancement due to the absorption of the chromophore moieties at 532 nm, we calculated their d_{33} values by using the approximate two-level model (Table 1), and the trend of curve C in Fig. 4 was similar as that of curves A and B.

To further study the influence of the increase in the size of the isolation groups, the order parameter (Φ) of the polymers (Table 1 and Fig. 6) was measured, which was calculated from the change of the UV-vis spectra of their films before and after corona poling under electric field, according to the equation described in Table 1 (footnote i). Coinciding well with the changing trend of observed in the tested values, the Φ value of the polymers also did not increase

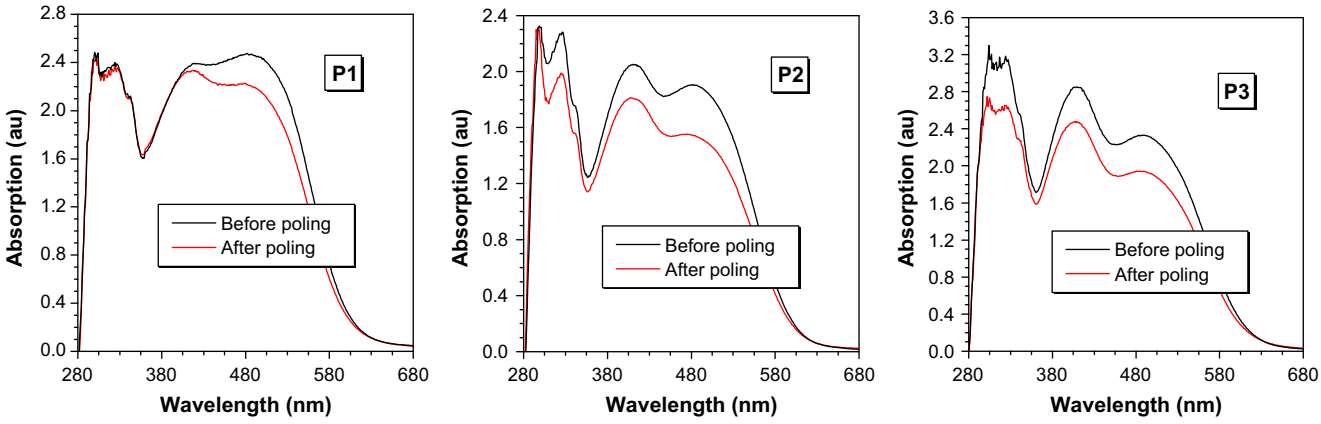

Fig. 6. Absorption spectra of the film of **P1–3** before and after poling.

with the size of isolation groups enlarging, further confirming the above discussion from another side.

The dynamic thermal stabilities of the NLO activities of the polymers were investigated by depoling experiments, in which the real time decays of their SHG signals were monitored as the poled films were heated from 35 to 150 °C in air at a rate of 4 °C/min. As shown in Fig. 7, the long-term temporal stability of the polymers was good, especially for **P2** and **P3**, of which the onset temperature for decays in the d_{33} values were as high as 130 °C, making them good candidates for the practical applications. Moreover, the results demonstrated that the introduction of the large size of the isolated groups to the chromophores benefited the thermal stability of the resultant polymers. Here, when the isolation spacers were changed from **Ph** to **BOP** (**Car**), the onset temperature was raised up to around 30 °C. On the other hand, as we discussed above on their d_{33} values, the d_{33} value of **P2** was 1.34 times higher than that of **P1.** Thus, based on our previous work [26–30], we may presume that by applying the concept of "suitable isolation groups", the "nonlinearity-stability trade off" could be solved somewhat.

4. Conclusion

Totally, in order to confirm the strange phenomena in our previous work, a new series of PVK-based NLO polymers containing nitro-based chromophores were successfully prepared, in which different size of isolation groups was linked to the chromophore moieties at the donor side to adjust their subtle structure, by applying the concept of "suitable isolation groups". Similar to our previous work, the resultant polymers exhibited relatively larger d_{33} values (up to 39.6 pm/V), good long-term temporal stability, as well as improved optical transparency and processibility, making them good candidates for the practical applications. In addition, the enhanced nonlinearity and thermal ability demonstrated that by introducing suitable isolation groups, the "nonlinearity–stability trade off" may be alleviated.

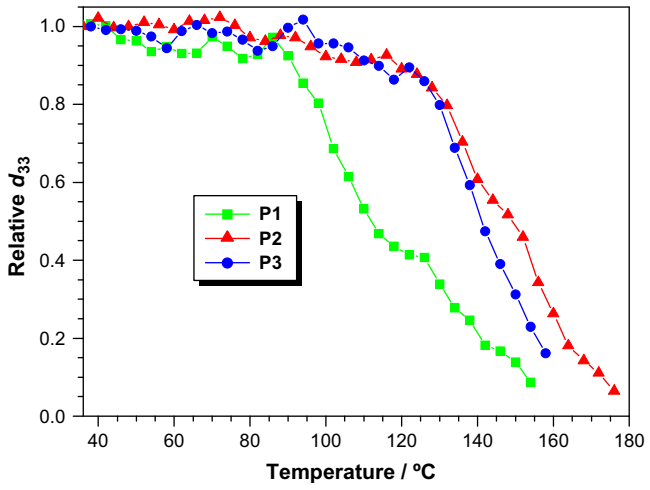

Fig. 7. Decay curves of SHG coefficient of **P1–3** as a function of temperature.

Acknowledgements

We are grateful to the National Science Foundation of China (No. 20674059, J0730426), the Program for NCET, the National Fundamental Key Research Program and Hubei Province for financial support.

References

[1] Moerner WE, Silence SM. Chem Rev 1994;94:127.
[2] Meerholz K, Volodin BL, Kippelen B, Peyghambarian N. Nature 1994;371:497.
[3] Zhang YD, Burzynski R, Ghosal S, Casstevens MK. Adv Mater 1996;8:111.
[4] Grazulevicius JV, Strohriegl P, Pielichowski J, Pielichowski K. Prog Polym Sci 2003;28:1297.
[5] Brar AS, Kaur S. J Polym Sci Part A Polym Chem 2006;44:1745.
[6] Kido J, Shionoya H, Nagai K. Appl Phys Lett 1995;67:2281.
[7] Xie XN, Deng M, Xu H, Yang SW, Qi DC, Gao CY, et al. J Am Chem Soc 2006;128:2738.
[8] Steenwinckel DV, Hendrickx E, Persoons A. Chem Mater 2001;13:1230.
[9] Feng M, Chen Y, He N, Gu LL, Gao LL, Hu Z, et al. J Polym Sci Part A Polym Chem 2008;46:5702.
[10] Yoon KR, Ko S-O, Lee SM, Lee H. Dyes and Pigments 2007;75:567.
[11] Yu D, Gharavi A, Yu LP. J Am Chem Soc 1995;117:11680.
[12] Woo HY, Shim HK, Lee K-S. Macromol Chem Phys 1998;199:1427.
[13] Zhang C, Wang C, Dalton LR, Zhang H, Steier WH. Macromolecules 2001;34:253.
[14] Zhang YD, Hokari H, Wada T, Shang YM, Marder SR, Sasabe H. Tetrahedron Lett 1997;38:8721.
[15] Zeng H, Zhan C, Qin J, Liu DY. Chem J Chin Univ 1995;16:206.
[16] Luo J, Qin J, Kang H, Ye C. Chem Mater 2001;13:927.
[17] Robinson BH, Dalton LR. J Phys Chem A 2000;104:4785.
[18] Pereverzev YV, Prezhdo OV, Dalton LR. Chem Phys Chem 2004;5:1821.
[19] (a) Ma H, Liu S, Luo J, Suresh S, Liu L, Kang SH, et al. Adv Funct Mater 2002;12:565;
(b) Fusco S, Centore R, Riccio P, Quatela A, Stracci G, Archetti G, et al. Polymer 2008;49:186;
(c) Yesodha SK, Pillai CKS, Tsutsumi N. Prog Polym Sci 2004;29:45.
[20] Liao Y, Anderson AA, Sullivan PA, Akelaitis AJP, Robinson BH, Dalton LR. Chem Mater 2006;18:1062.
[21] Sullivan PA, Akelaitis AJP, Lee SK, McGrew G, Choi DH, Dalton LR. Chem Mater 2006;18:344.
[22] Ma H, Chen BQ, Sassa T, Dalton LR, Jen AKY. J Am Chem Soc 2001;123:986.
[23] Luo J, Liu S, Haller M, Liu L, Ma H, Alex JKY. Adv Mater 2002;14:1763.

[24] Fréchet JMJ, Henmi M, Gitsov I, Aoshima S, Leduc MR, Grubbs RB. Science 1995;269:1080.
[25] Fréchet JMJ, Hawker CJ, Gitsov I, Leon JWJ. Macromol Sci Pure Appl Chem 1996;33:1399.
[26] Li Z, Li Z, Di C, Zhu Z, Li Q, Zeng Q, et al. Macromolecules 2006;39:6951.
[27] Li Z, Zeng Q, Li Z, Dong S, Zhu Z, Li Q, et al. Macromolecules 2006;39:8544.
[28] Zeng Q, Li Z, Li Z, Ye C, Qin J, Tang BZ. Macromolecules 2007;40:5634.
[29] Li Z, Li P, Dong S, Zhu Z, Li Q, Zeng Q, et al. Polymer 2007;47:3650.
[30] Li Z, Dong S, Yu G, Li Z, Liu Y, Ye C, et al. Polymer 2007;47:5520.
[31] Li Z, Zeng Q, Yu G, Li Z, Ye C, Liu Y, et al. Macromol Rapid Commun 2008; 29:136.
[32] Li Z, Yu G, Li Z, Liu Y, Ye C, Qin J. Polymer 2008;49:901.
[33] Li Q, Li Z, Ye C, Qin J. J Phys Chem B 2008;112:4928.
[34] Li Q, Yu G, Huang J, Liu H, Li Z, Ye C, et al. Macromol Rapid Commun 2008;29:798.
[35] Li Q, Li Z, Zeng F, Gong W, Li Z, Zhu Z, et al. J Phys Chem B 2007;111:508.
[36] Li Z, Dong S, Li P, Li Z, Liu Y, Ye C, et al. J Polym Sci Part A Polym Chem 2008;46:2983.
[37] Miyaura N, Suzuki A. Chem Rev 1995;95:2457.
[38] Cheuk KKL, Lam JWY, Lai LM, Dong Y, Tang BZ. Macromolecules 2003; 36:5947.
[39] Luo J, Haller M, Li H, Tang H-Z, Jen AKY. Macromolecules 2004;37:248.
[40] Li Z, Huang C, Hua J, Qin J, Yang Z, Ye C. Macromolecules 2004;37:371.
[41] Li Z, Qin J, Li S, Ye C, Luo J, Cao Y. Macromolecules 2002;35:9232.
[42] Li Z, Gong W, Qin J, Yang Z, Ye C. Polymer 2005;46:4971.
[43] Li Z, Hua J, Li Q, Huang C, Qin A, Ye C, et al. Polymer 2005;46:11940.
[44] Li Z, Li J, Qin J, Qin A, Ye C. Polymer 2005;46:363.